DEPARTMENT OF ELECTRICAL ENGINEERING TECHNOLOGY
COLLEGE OF ENGINEERING AND TECHNOLOGY
OLD DOMINION UNIVERSITY
NORFOLK, VIRGINIA 23529-0243

ANALYSIS OF RADIOMETER CALIBRATION EFFECTS WITH TOUCHSTONE

By

William D. Stanley, Principal Investigator

Final Report
For the period June 22, 1989 to December 31, 1989

Prepared for the
National Aeronautics and Space Administration
Langley Research Center
Hampton, Virginia 23665-5225

Under
Master Contract Agreement NAS-1-18584
Task Authorization No. 63
Chase P. Hearn, Technical Monitor
FED-Antenna and Microwave Research Branch

Submitted by the
Old Dominion University Research Foundation
P.O. Box 6369
Norfolk, Virginia 23508-0369

March 1990

DEPARTMENT OF ELECTRICAL ENGINEERING TECHNOLOGY
COLLEGE OF ENGINEERING AND TECHNOLOGY
OLD DOMINION UNIVERSITY
NORFOLK, VIRGINIA 23529-0243

ANALYSIS OF RADIOMETER CALIBRATION EFFECTS WITH TOUCHSTONE

By

William D. Stanley, Principal Investigator

Final Report
For the period June 22, 1989 to December 31, 1989

Prepared for the
National Aeronautics and Space Administration
Langley Research Center
Hampton, Virginia 23665-5225

Under
Master Contract Agreement NAS-1-18584
Task Authorization No. 63
Chase P. Hearn, Technical Monitor
FED-Antenna and Microwave Research Branch

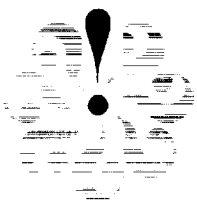

March 1990

ANALYSIS OF RADIOMETER CALIBRATION EFFECTS WITH TOUCHSTONE

By

William D. Stanley*

ABSTRACT

The microwave circuit analysis program TOUCHSTONE is used to study two effects of importance in radiometer calibration. The two effects are impedance mismatches at the antenna-air and cold load-air interfaces and dissipatives losses, which radiate thermal noise into the system. The results predicted by TOUCHSTONE are shown to be in very close agreement with earlier results obtained by purely analytical methods. The techniques used in establishing the circuit models and in processing the resulting data are described in detail.

*Chairman, Department of Electrical Engineering Technology, Old Dominion University, Norfolk, Virginia 23529-0243.

TABLE OF CONTENTS

LIST OF TABLES

LIST OF FIGURES

TABLE OF CONTENTS (Concluded)

LIST OF FIGURES (Concluded)

INTRODUCTION

Two phenomena of considerable interest in radiometer remote-sensing systems are those that arise from (a) multiple reflections and (b) dissipative losses. Both phenomena may produce errors in either the reference calibration process or in an operational mode. Analytical methods are very cumbersome to apply and often do not provide an intuitive insight into the process involved.

In an effort to provide an alternate approach to this problem, the possibility of computer modeling of the phenomena has been investigated. In particular, the program TOUCHSTONE has been used with much success. TOUCHSTONE is a trademark of *EESOF, Inc., and it is a comprehensive microwave analysis program providing features for modeling both discrete and distributed parameter high frequency and microwave systems.

Complete operational details of TOUCHSTONE are provided in a user's manual, and they are too unwieldy to attempt a summary coverage in this report [reference 1]. Instead, the emphasis here will be directed toward the development of the circuit forms that may be represented with various TOUCHSTONE models and how they may be related to actual radiometer circuit behavior. Some data obtained from an actual radiometer system will be analyzed, and the results will be compared with an earlier analysis performed on that particular system.

Two effects to be delineated in this study are the representation of mismatches and the representation of dissipative losses. The first effect can be achieved with transformer models, and the second effect can be

*EESOF, Inc.
31194 Albania Drive
Westlike Village, CA 91362

achieved with resistors coupled to the system with transformers. The various S parameters can be determined and related to the power transmission coefficients for the signal, the dissipative losses, and system mismatches. A radiometer calibration system containing multiple reflections will be analyzed in detail.

SIMULATION OF A MISMATCH

All measurements with TOUCHSTONE are based on the assumption that each port is terminated in a reference resistive characteristic impedance. The default impedance is $Z_o = R_o = 50\ \Omega$, although this value may be changed if necessary.

A desired mismatch may be introduced at any port by using a transformer to couple between the port and the remainder of the system as illustrated in Figure 1. Let Γ represent the desired reflection coefficient at the given port, and assume a reference characteristic impedance of 50 Ω. The input impedance Z_{in} as seen at the load must be such that

$$\frac{50 - Z_{in}}{50 + Z_{in}} = \Gamma \qquad (1)$$

This leads to

$$Z_{in} = \frac{50\ (1-\Gamma)}{1 + \Gamma} \qquad (2)$$

Assuming that the characteristic impedance of any component connected to the right-hand side of the transformer is 50 Ω, the turns ratio N must satisfy

$$50N^2 = Z_{in} = \frac{50\ (1-\Gamma)}{1 + \Gamma} \qquad (3)$$

which leads to

$$N = \sqrt{\frac{1 - \Gamma}{1 + \Gamma}} \tag{4}$$

Either the value given by (4) or its reciprocal will be satisfactory. The latter case refers to a reversal in the sign of the reflection coefficient, but the magnitude is the same.

SIMULATION OF DISSIPATIVE LOSS

Dissipative loss in a transmission system may be modeled with a symmetrical T-pad attenuator. Assume under matched conditions that the network power ratio may be defined as

$$\frac{P_{in}}{P_{out}} = e^{2\alpha} \tag{5}$$

where P_{in} and P_{out} are the respective input and output values and α is the attenuation constant. It can be shown with image parameter theory that this attenuation can be simulated with the circuit of Figure 2.

The available thermal noise power P_{av} of any resistance R is given by

$$P_{av} = kTB \tag{6}$$

where k = Boltzmann's constant = 1.38×10^{-23} J/K, T is the absolute temperature in Kelvin, and B is the bandwidth in hertz. When the input and output ports of the circuit are terminated in the characteristic or image impedance, the output noise power P_{no} is given by

$$P_{no} = G_{av}\, kTB = G_{av}\, P_{av} \tag{7}$$

where G_{av} is the available gain relating the maximum available output power to the power available from the resistance.

Next, consider the T-pad attenuator of Figure 3(a), and note that this circuit can be realized with three transformers as shown in (b). The turns ratio of the various transformers must satisfy

$$\frac{50}{N_1^2} = R_1 \tag{8}$$

and

$$\frac{50}{N_2^2} = R_2 \tag{9}$$

which leads to

$$N_1 = \sqrt{\frac{50}{R_1}} \tag{10}$$

$$N_2 = \sqrt{\frac{50}{R_2}} \tag{11}$$

Denote the three ports corresponding to the three resistors with the subscripts "1", "2", and "3", and denote the input and output ports with the subscripts "i" and "o", respectively. Let S_{01}, S_{02}, and S_{03}, represent the scattering parameters relating the transmission between ports 1, 2, and 3, and the output. The net available output noise power P_{no} is given by

$$P_{no} = |S_{01}|^2 kT_1B + |S_{02}|^2 kT_2B + |S_{03}|^2 kT_3B$$

where T_1, T_2, and T_3 are the temperatures of the three resistances, respectively. The net output noise temperature T_{no} resulting from the three resistances can be expressed as

$$T_{no} = \frac{P_{no}}{kB} = |S_{01}|^2 T_1 + |S_{02}|^2 T_2 + |S_{03}|^2 T_3 \tag{13}$$

Next, assume that $T_1 = T_2 = T_3 = T_p$, in which case

$$T_{no} = \left[|S_{01}|^2 + |S_{02}|^2 + |S_{03}|^2 \right] T_p \tag{14a}$$

$$= |d|^2 T_p \tag{14b}$$

where

$$|d|^2 = |S_{01}|^2 + |S_{02}|^2 + |S_{03}|^2 \tag{15}$$

The quantity $|d|^2$ is the dissipation factor for the network, and it is the weighting factor that determines the contribution to the output noise through loss from the physical temperature T_p. From the preceding analysis, it can be deduced that a knowledge of S_{01}, S_{02}, and S_{03} may be determined with TOUCHSTONE. Further, the use of the processing function permits the square of the magnitude to be determined within the program.

REDUCTION IN NUMBER OF ATTENUATOR PORTS

Realization of the attenuation network with three resistors obviously requires three separate ports in addition to input and output ports. A procedure will now be developed for eliminating one of the ports by means of an impedance transformation of the original circuit.

Referring to the T-pad of Figure 3(a), the open circuit impedance matrix [Z] can be expressed as

$$[Z] = \begin{bmatrix} R_1 + R_2 & R_2 \\ R_2 & R_1 + R_2 \end{bmatrix} \tag{16}$$

The impedance level of the network at the input can be multiplied by a constant 1/N multiplying both the first row and the first column by 1/N. The modified matrix [Z]' is then expressed as

$$[Z]' = \begin{bmatrix} \dfrac{(R_1 + R_2)}{N^2} & \dfrac{R_2}{N} \\ \dfrac{R_2}{N} & R_1 + R_2 \end{bmatrix} \tag{17}$$

Assume next that it is desired to realize [Z]' as an L-network with the first element on the left as the series element. For this to be possible, the following equality must be satisfied:

$$\frac{R_2}{N} = R_1 + R_2 \tag{18}$$

or

$$N = \frac{R_2}{R_1 + R_2} \tag{19}$$

To compensate, an ideal transformer with turns ratio N/1 from primary to secondary must be placed at the input. The resulting circuit, after calculation of the two resistance values, is shown in Figure 4.

To simulate the circuit with TOUCHSTONE, two additional transformers are required to transform the 50-Ω terminations to the values of the two resistances. The resulting form is shown in Figure 5. The values of N_A, N_B, and N_C must satisfy

$$N_A = \frac{R_2}{R_1 + R_2} \tag{20}$$

$$\frac{50}{N_B^2} = \frac{R_1(R_1 + R_2)\ (R_1 + 2R_2)}{R_2^2} \tag{21}$$

or

$$N_B = \frac{\sqrt{50}\ R_2}{\sqrt{R_1(R_1 + R_2)\ (R_1 + 2R_2)}} \tag{22}$$

$$\frac{50}{N_C^2} = R_1 + R_2 \tag{23}$$

$$N_C = \frac{\sqrt{50}}{\sqrt{R_1 + R_2}} \tag{24}$$

Although many different attenuation values were considered in this study, the preceding process is illustrated for a representative case in Figure 6. A T-pad attenuator producing an insertion loss of 1 dB is shown in (a). The circuit of (b) represents a TOUCHSTONE model employing three dissipation ports. By employing the transformation previously described, the circuit is reduced to one having two resistances as shown in (c). Finally, the TOUCHSTONE realization is shown in (d).

CALIBRATION SYSTEM

The basic system configuration for calibration of a noise-injection radiometer is shown in Figure 7. A cold load at temperature T_L is located at a distance d from the radiometer. In most cases of interest, this load is cooled to the temperature of liquid nitrogen, in which case T_L = 77 K.

A closed-loop feedback noise-balancing Dicke radiometer has been assumed. Injected noise is added to the input noise such that the mean noise power levels on the two halves of the Dicke Cycle are equal. The physical temperature of the radiometer is denoted as T_p, of which a typical value is T_p = 308 K. Various transmission line models of the calibration system have been considered in an earlier report [reference 2]. Equations were derived for representing the combined effects of the mismatches at the cold load-air interface and the antenna-air interface. In this report, these models will be simulated with TOUCHSTONE.

SIMULATION CASES

In order to provide a comparison with results obtained through purely analytical methods, some actual data considered in an earlier report were used [reference 2]. The values assumed are

Antenna Reflection Coefficient = 0.141 (-17dB)

Cold Load Reflection Coefficient = 0.05 (-26dB)

Cold Load Temperature = 77 K

Reference Physical Temperature = 308 K

Several different radiometer configurations were considered. The different configurations, along with the TOUCHSTONE file names, are as follows:

RADMET1: lossless system without a circulator

RADMET2: lossless system with a circulator

RADMET3: lossy system without a circulator

RADMET4: lossy system with a circulator

In an actual radiometer, the variation of measured temperature is normally observed as a spatial function of the distance between the load and the antenna. With TOUCHSTONE, however, it is easier to maintain a constant spacing and vary the frequency since the observed results are the same. The path length was established as a one-eighth wavelength at a frequency at 1 GHz.

As a comparison of the different models, various runs were obtained, and certain variables were determined and tabulated. The runs are summarized in Table 1. The following quantities are defined:

$|t|^2$ - power transmission coefficient from input to output (or transducer gain)

$|t_C|^2$ - power transmission coefficient from input to output

$|d|^2$ - power dissipation function

$|\gamma_o|^2$ - net output power reflection coefficient

The net output temperature T_{out} is given by

$$T_{out} = |t|^2 T_L + |t_C|^2 T_C + |d|^2 T_p + |\gamma_o|^2 T_R \qquad (25)$$

where T_{out} is the net output temperature, T_L is the load temperature, T_C is the circulator temperature, T_P is the physical temperature of the dissipation losses and T_R is the reverse temperature radiated back toward the antenna junction by the radiometer.

The variations in each of the power coefficients were observed over a frequency range encompassing at least one full cycle. The maximum and minimum values of these quantities are denoted with the subscripts "max" and "min", respectively. The first configuration considered was a lossless system without a circulator (RADMET1), and the layout in shown in Figure 8. Since there is neither a circulator nor dissipative loss, no data appear under those applicable columns. It turns out that the maximum value of the transmission coefficient occurs at the same point as the minimum value of the output reflection coefficient and vice-versa.

The second configuration considered was a lossless system with a circulator (RADMET2), and the layout is shown in Figure 9. The maximum and minimum values of the pertinent data are shown in the second row of Table 1.

The presence of the circulator results in $\gamma_o = 0$; i.e., the reverse radiation is diverted into the circulator terminating resistor. However, noise generated by the circulator termination propagates toward the antenna and is reflected back into the radiometer. Consequently, the values of $|t_C|^2_{,max}$ and $|t_C|^2_{,min}$ in this case are exactly the same as for $|\gamma_o|^2_{,max}$ and $|\gamma_o|^2_{,min}$ for the preceding case.

A conclusion that can be drawn from the preceding discussion is that there is no advantage gained from placing a circulator in the front end of the radiometer if the circulator termination is at the same physical temperature as the radiometer. Indeed, if there is any loss or mismatch produced by the circulator, the system may be further degraded. However, if the circulator is nearly ideal, and if its termination can be cooled to a lower temperature, some advantage could be gained.

The third configuration considered was a lossy system without a circulator (RADMET3), and the layout is shown in Figure 10. At this particular point in the analysis, a loss of 1 dB is assumed. (Later, the results of varying the loss will be considered.) The maximum and minimum values of the data obtained are shown in the third row of Table 1. The presence of dissipative losses results in a non-zero value for $|d|^2$. It turns out that the maximum value of $|t|^2$ corresponds to minimum values of $|d|^2$ and $|\gamma_o|^2$ and vice versa.

The fourth configuration considered was a lossy system with a circulator (RADMET4), and the layout is shown in Figure 11. As in the preceding case, a loss of 1 dB is assumed at this time. The maximum and minimum values of the data obtained are shown in the fourth row of Table 1. As in the lossless case, the output reflection coefficient is now zero, but the circulator termination now contributes to the output, and the weight of this contribution is the same as for the output reflection function when no circulator is used.

DISSIPATIVE LOSS EFFECTS

A study was made to determine the net output temperature as a function of dissipative loss. Although either RADMET3 (without circulator) or RADMET4 (with circulator) could be used, the former was chosen because it has one less port in the simulation. As a prelude to the analysis, values of the various parameters required to simulate the transmission as a function of the decibel loss were calculated. The results are tabulated in Table 2.

The results of various simulations with RADMET3 are provided in Table 3. As indicated earlier, the maximum value of $|t|^2$ occurs at the minimum values of $|d|^2$ and vice versa. Further, the only difference in the

results that would be obtained with RADMET4 is that the values listed under the $|\gamma_o|^2$ columns would be transferred to the $|t_C|^2$ columns.

After the preceding data were obtained, various temperature parameters were calculated and tabulated in Table 4. The definitions of these quantities are listed as follows:

T_L = cold load temperature; i.e., the temperature that should be measured

T_{max} = maximum temperature as sensed by radiometer

T_{min} = minimum temperature as sensed by radiometer

$\bar{T}_{meas}$ = mean value of measured temperature

T_{bias} = fixed bias error in measurement

T_{var} = peak value of variable component of error in measurement

Formulas for determining the preceding quantities are the following:

$$\bar{T}_{meas} = \frac{T_{max} + T_{min}}{2} \tag{25}$$

$$T_{bias} = \bar{T}_{meas} - 77 \tag{26}$$

$$T_{var} = \frac{T_{max} - T_{min}}{2} \tag{27}$$

A comparison between all points common to this study and the earlier analytical study [reference 2] is given in Table 5. The results of the earlier study were based on a few simplifying assumptions in the final form of the equation, so perfect agreement is not expected. However, it is obvious that the results are very close to each other and differ by less than 1% in all cases.

TABLES

	$\|t\|^2_{,max}$	$\|t\|_{,max}$	$\|t_C\|^2_{,max}$	$\|t_C\|^2_{,min}$	$\|d\|^2_{,max}$	$\|d\|^2_{,min}$	$\|\gamma_o\|^2_{,max}$	$\|\gamma_o\|^2_{,min}$
LOSSLESS W/O CIRC (Fig. 8)	0.991	0.964					0.036	8.5×10^{-3}
LOSSLESS W/ CIRC (Fig. 9)	0.991	0.964	0.036	8.5×10^{-3}			0	0
LOSSY W/O CIRC (Fig. 10)	0.788	0.766			0.212	0.207	0.023	5.4×10^{-3}
LOSSY W/ CIRC 1 dB (Fig. 11)	0.788	0.766	0.023	5.4×10^{-3}	0.212	0.207	0	0

Table 1. Comparison of different radiometer simulation configurations.

LOSS	R_1, Ω	R_2, Ω	NA	NB	NC
0 dB	0	∞	1	∞	0
0.1 dB	0.2878	4343	0.9999	9.320	0.1073
0.2 dB	0.5756	2171	0.9997	6.589	0.1517
0.3 dB	0.8634	1447	0.9994	5.379	0.1858
0.4 dB	1.1511	1085	0.9989	4.659	0.2146
0.5 dB	1.439	868.1	0.9983	4.163	0.2398
0.6 dB	1.726	723.2	0.9976	3.799	0.2626
0.7 dB	2.014	619.7	0.9968	3.515	0.2836
0.8 dB	2.303	542.1	0.9958	3.284	0.3031
0.9 dB	2.588	481.7	0.9947	3.096	0.3213
1.0 dB	2.875	433.3	0.9934	2.934	0.3386
1.5 dB	4.307	288.1	0.9853	2.383	0.4135
2.0 dB	5.731	215.2	0.9741	2.048	0.4757
2.5 dB	7.146	171.3	0.9600	1.814	0.5293
3.0 dB	8.550	141.9	0.9432	1.636	0.5765

Table 2. Attenuation network parameters as a function of insertion loss.

	$\|t\|^2_{,max}$	$\|t\|^2_{,max}$	$\|t_c\|^2_{,max}$	$\|t_c\|^2_{,min}$	$\|d\|^2_{,max}$	$\|d\|^2_{,min}$	$\|\gamma_o\|^2_{,max}$	$\|\gamma_o\|^2_{,min}$
0 dB								
0.1 dB	0.969	0.942			0.0234	0.0233	0.034	8.2×10^{-3}
0.2 dB	0.947	0.921			0.046	0.045	0.033	7.8×10^{-3}
0.3 dB	0.925	0.900			0.069	0.068	0.031	7.4×10^{-3}
0.4 dB	0.904	0.879			0.091	0.089	0.030	7.1×10^{-3}
0.5 dB	0.884	0.859			0.113	0.109	0.029	6.8×10^{-3}
0.6 dB	0.864	0.840			0.133	0.130	0.027	6.5×10^{-3}
0.7 dB	0.844	0.820			0.154	0.150	0.026	6.2×10^{-3}
0.8 dB	0.825	0.802			0.173	0.170	0.025	5.9×10^{-3}
0.9 dB	0.806	0.784			0.193	0.188	0.024	5.6×10^{-3}
1.0 dB	0.788	0.766			0.212	0.207	0.023	5.4×10^{-3}
2.0 dB	0.626	0.608			0.378	0.371	0.014	3.4×10^{-3}
3.0 dB	0.497	0.483			0.508	0.501	9.0×10^{-3}	2.1×10^{-3}

Table 3. Transmission and dissipation factors for lossy system without circulator as a function of insertion loss.

LOSS	T_L	T_{max}	T_{min}	$T_{max} - T_{min}$	$\bar{T}_{meas}$	T_{bias}	T_{var}
0 dB	77	85.32	78.93	6.39	82.13	5.13	3.20
0.1 dB	77	90.21	84.32	5.89	87.27	10.27	2.95
0.2 dB	77	95.25	89.18	6.07	92.22	15.22	3.04
0.3 dB	77	100.10	94.45	5.65	97.28	20.28	2.83
0.4 dB	77	104.95	99.21	5.74	102.08	25.08	2.87
0.5 dB	77	109.88	103.73	6.15	106.81	29.81	3.08
0.6 dB	77	113.96	108.57	5.39	111.27	34.27	2.70
0.7 dB	77	118.58	113.10	5.48	115.84	38.84	2.74
0.8 dB	77	122.74	117.70	5.04	120.22	43.22	2.52
0.9 dB	77	127.20	121.69	5.51	124.45	47.45	2.76
1.0 dB	77	131.36	126.10	5.26	128.73	51.73	2.63
2.0 dB	77	167.55	163.52	4.03	165.54	88.54	2.02
3.0 dB	77	196.43	196.15	4.28	194.29	117.29	2.14

Table 4. Temperature variables for lossy system as a function of insertion loss.

LOSS	$T_{max}^{(1)}$	$T_{max}^{(2)}$	% Diff	$T_{min}^{(1)}$	$T_{min}^{(2)}$	% Diff
0 dB	85.43	85.32	0.13	78.91	78.93	0.03
0.1 dB	90.49	90.21	0.31	84.13	84.32	0.23
0.5 dB	109.63	109.88	0.23	103.83	103.73	0.10
1.0 dB	131.20	131.36	0.12	126.03	126.10	0.06
2.0 dB	167.57	167.55	0.01	163.46	163.52	0.06
3.0 dB	196.45	196.43	0.01	193.19	192.15	0.54

(1) Earlier study [reference 2]
(2) TOUCHSTONE simulation

Table 5. Comparison of earlier analytical studies and TOUCHSTONE simulation studies at common points.

FIGURES

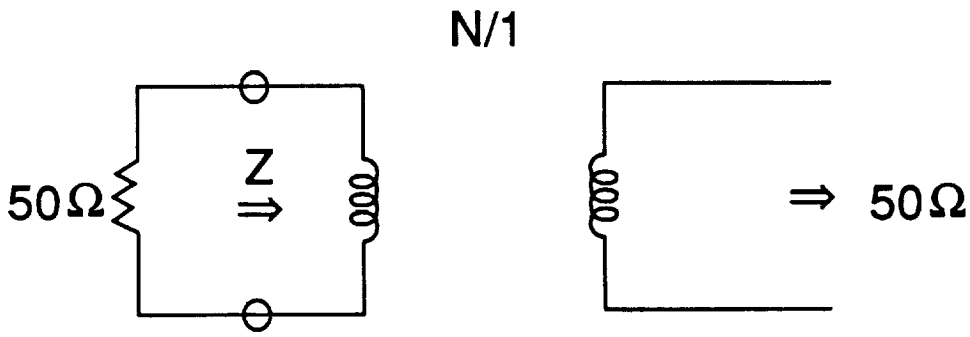

Figure 1. Creation of a mismatch at a port by use of a transformer.

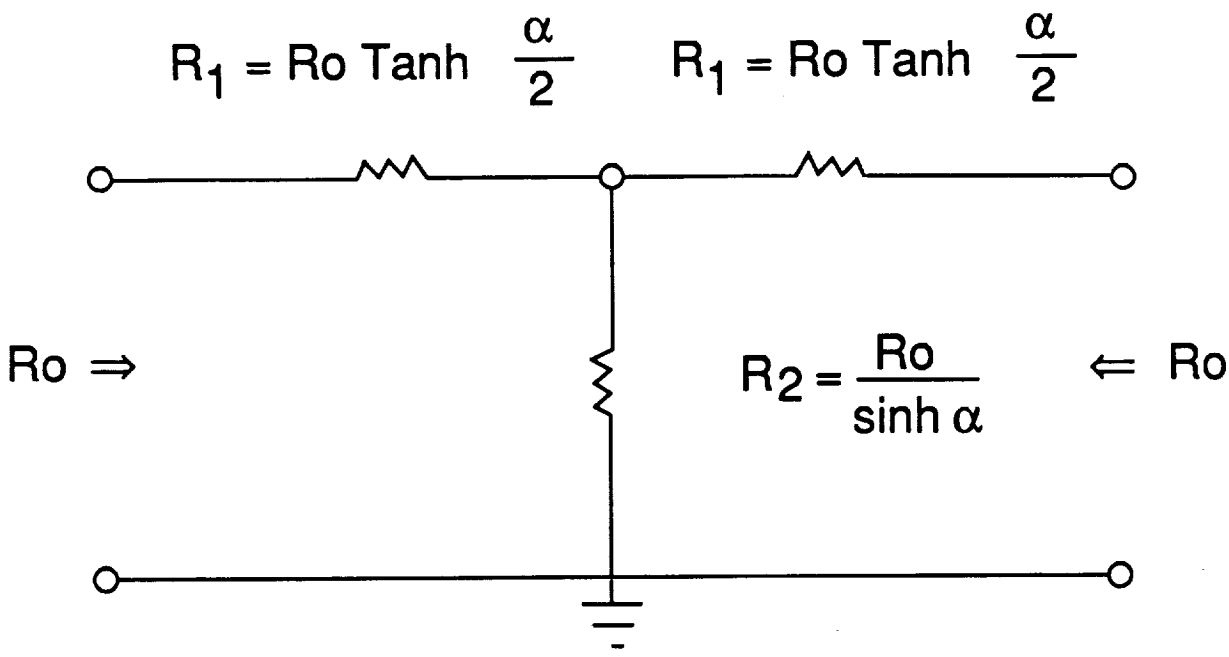

Figure 2. Matched T-pad attenuator network.

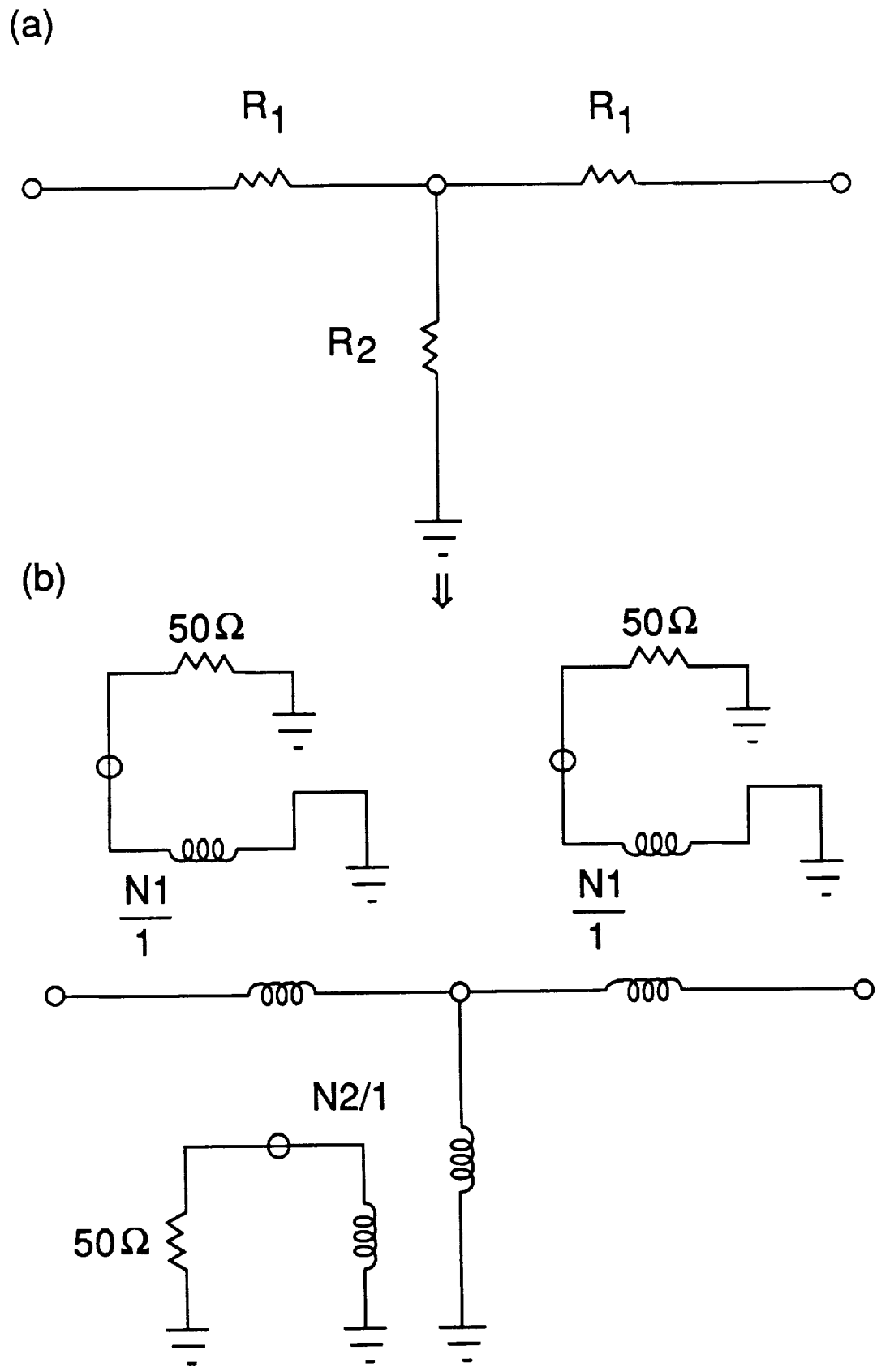

Figure 3. Simulation of a T-pad attenuator with TOUCHSTONE model components.

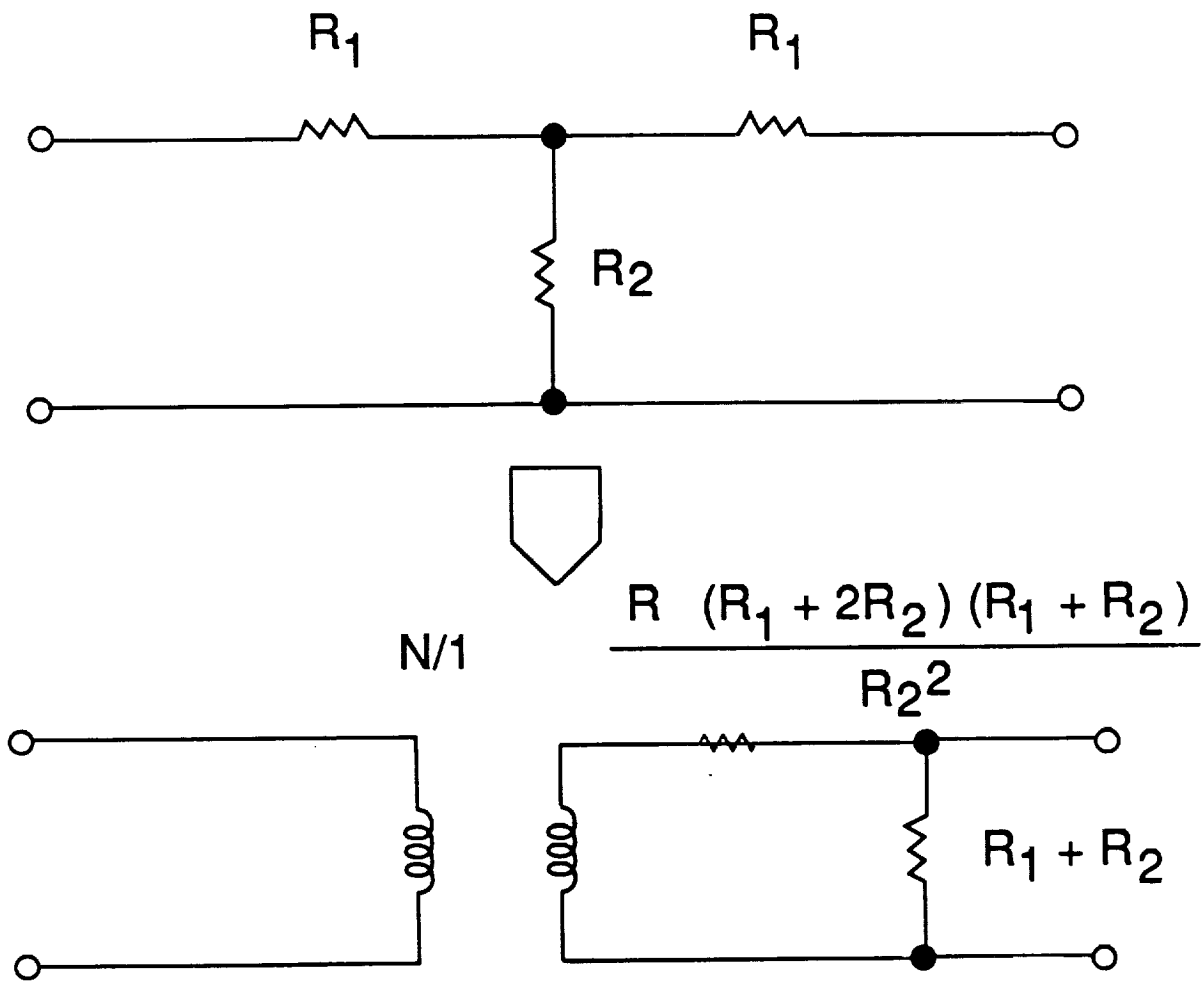

$$N = \frac{R_2}{R_1 + R_2}$$

Figure 4. Conversion of T-pad network to equivalent L-pad network with transformer.

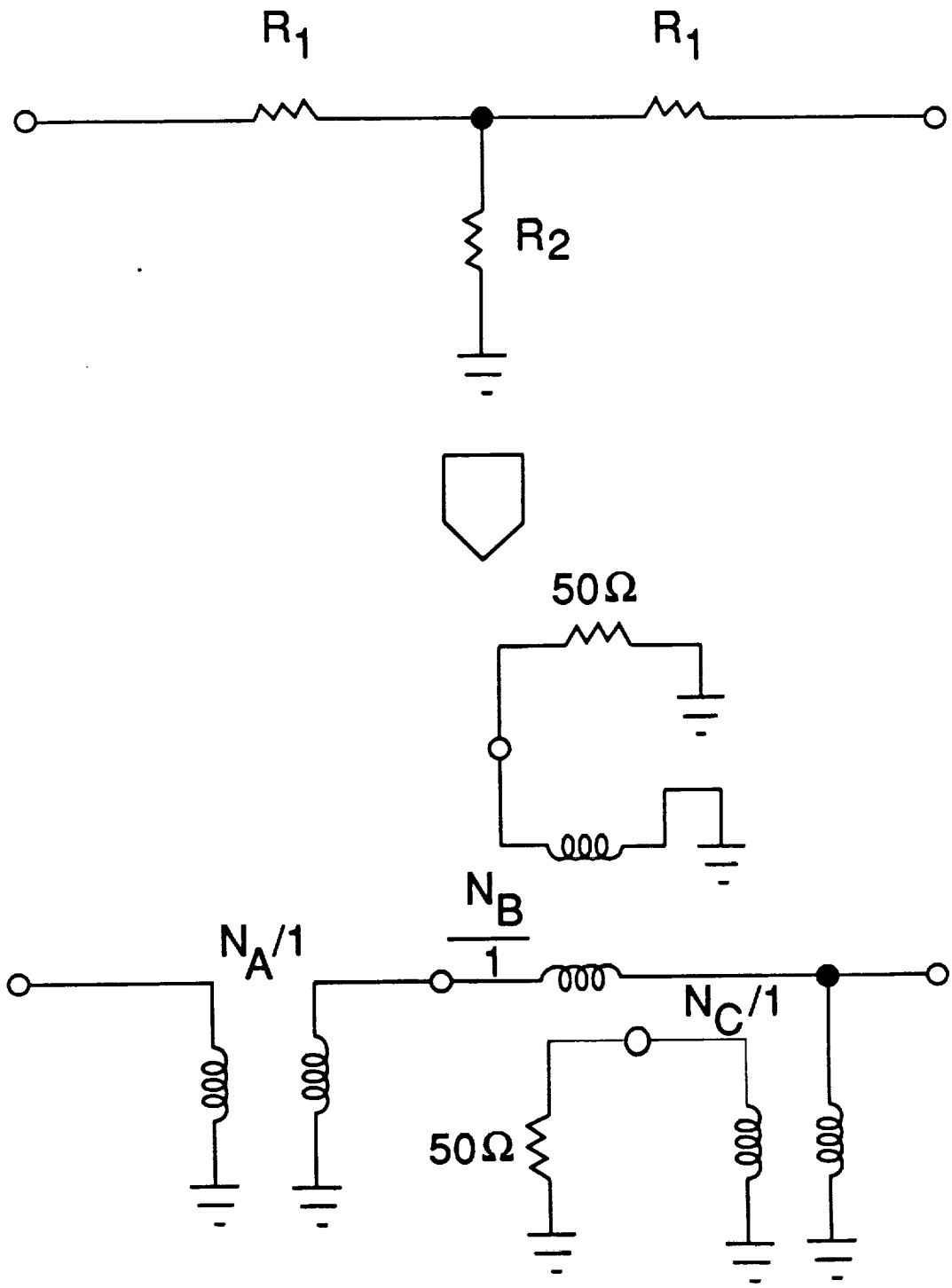

Figure 5. Conversion of T-pad attenuator to L-pad network with simulation using TOUCHSTONE components.

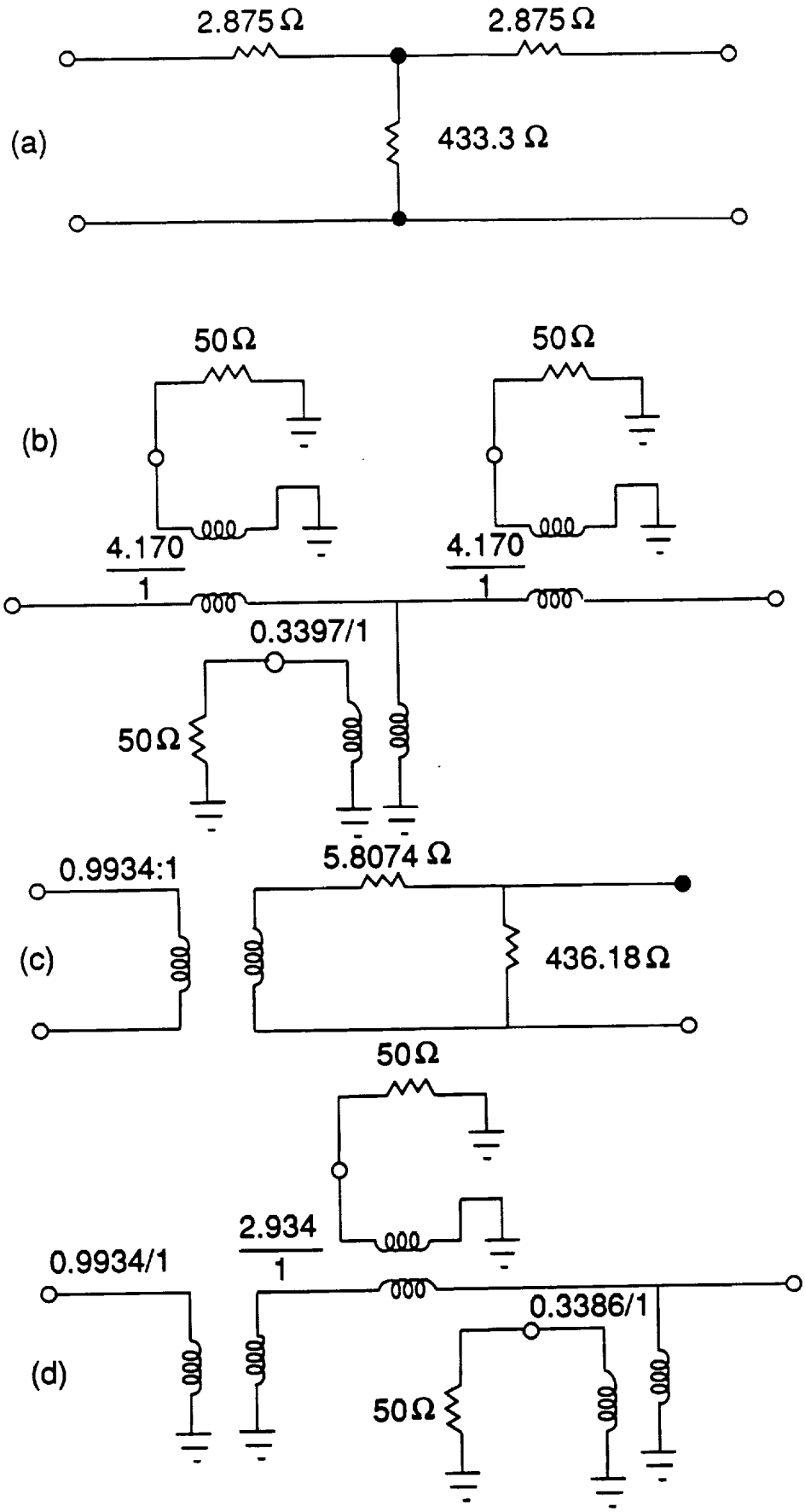

Figure 6. Representative attenuator circuit (1 dB) converted to two-port form.

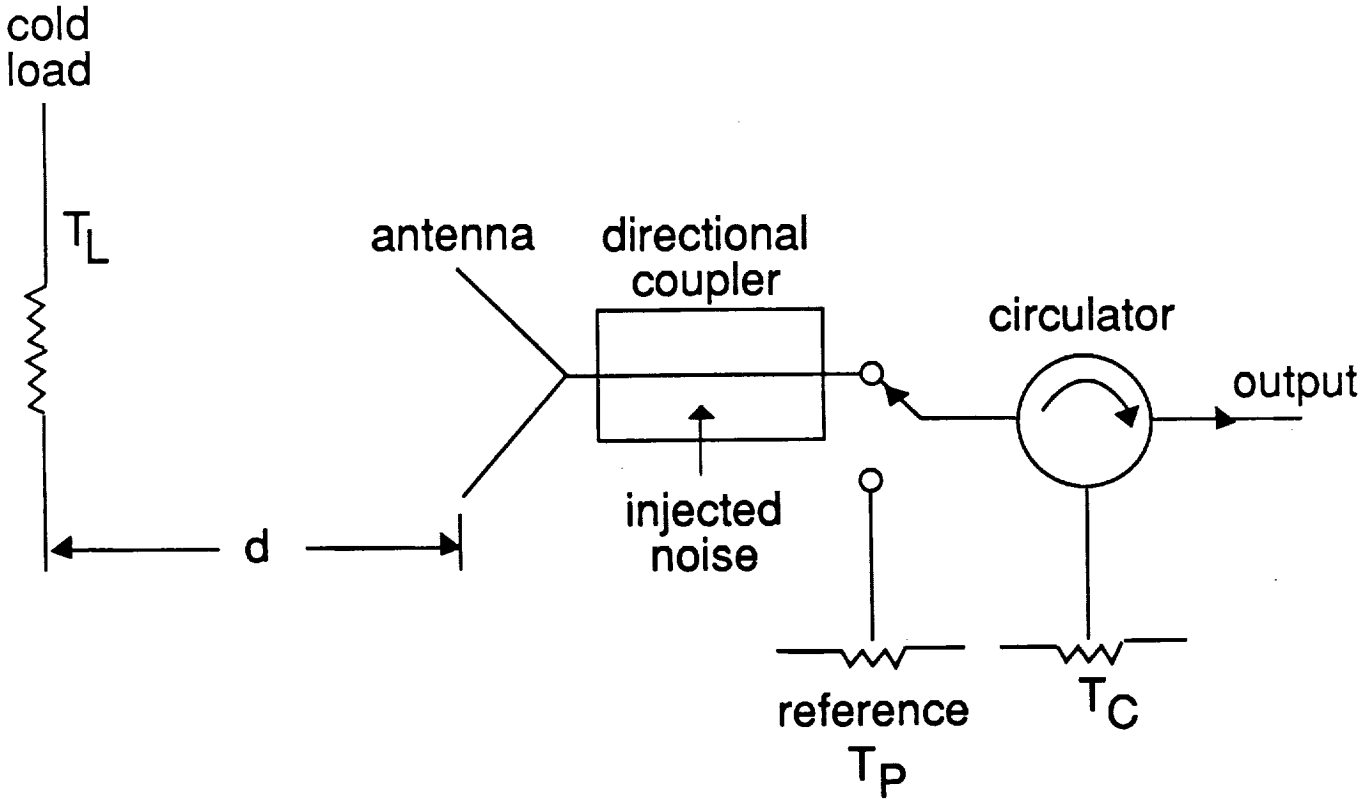

Figure 7. Basic radiometer system configuration for calibration.

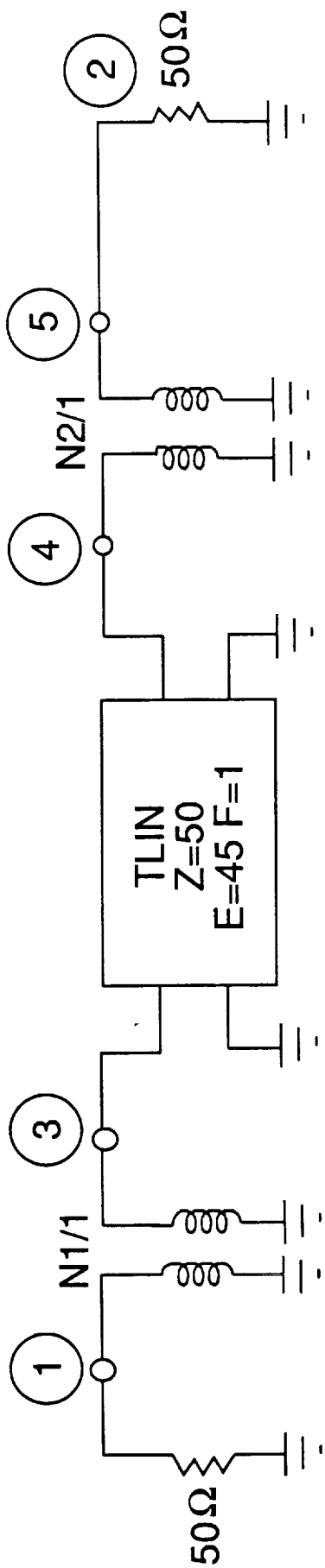

Figure 8. Two-port simulation of lossless calibration system without circulator.

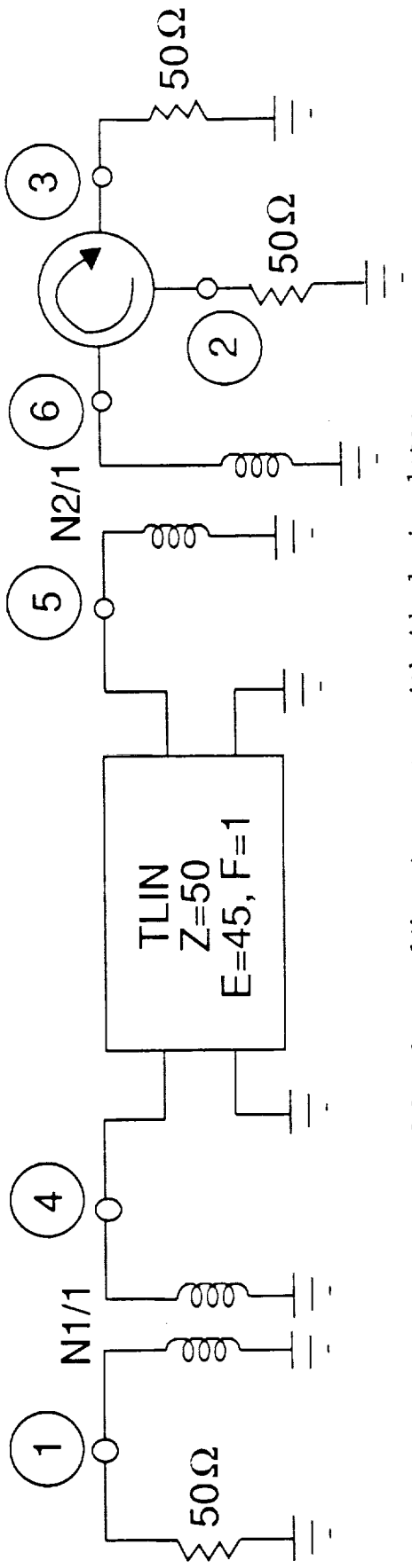

Figure 9. Three-port simulator of lossless calibration system with ideal circulator.

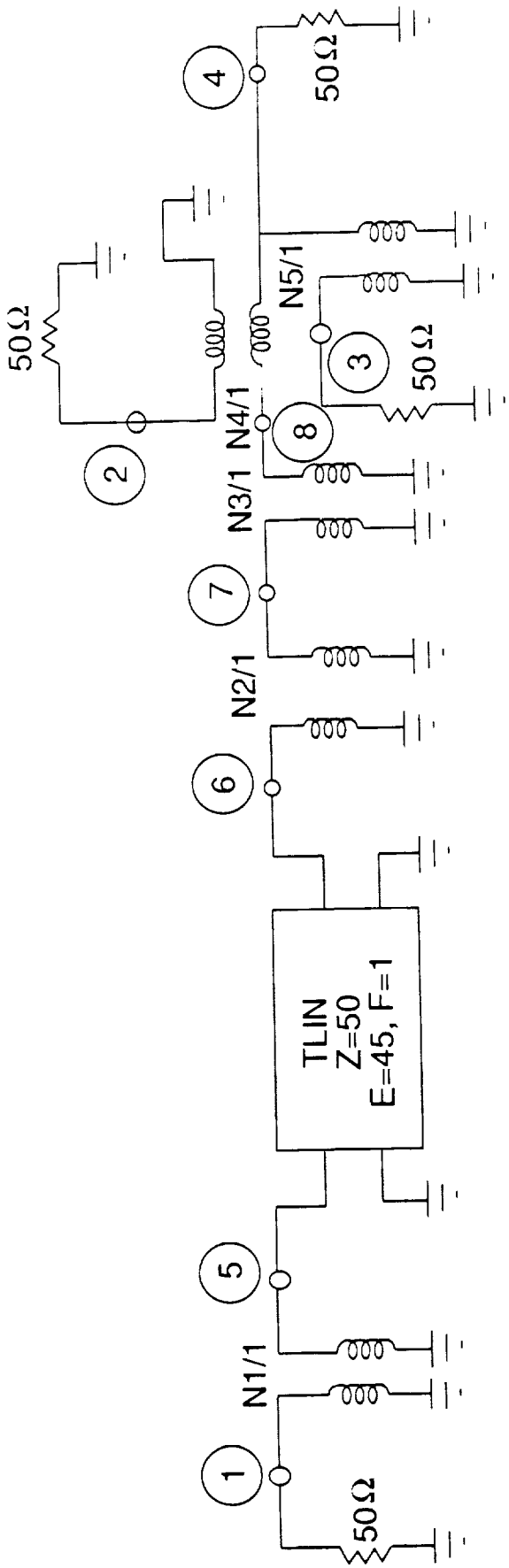

Figure 10. Four-port simulation of lossy calibration system without circulator.

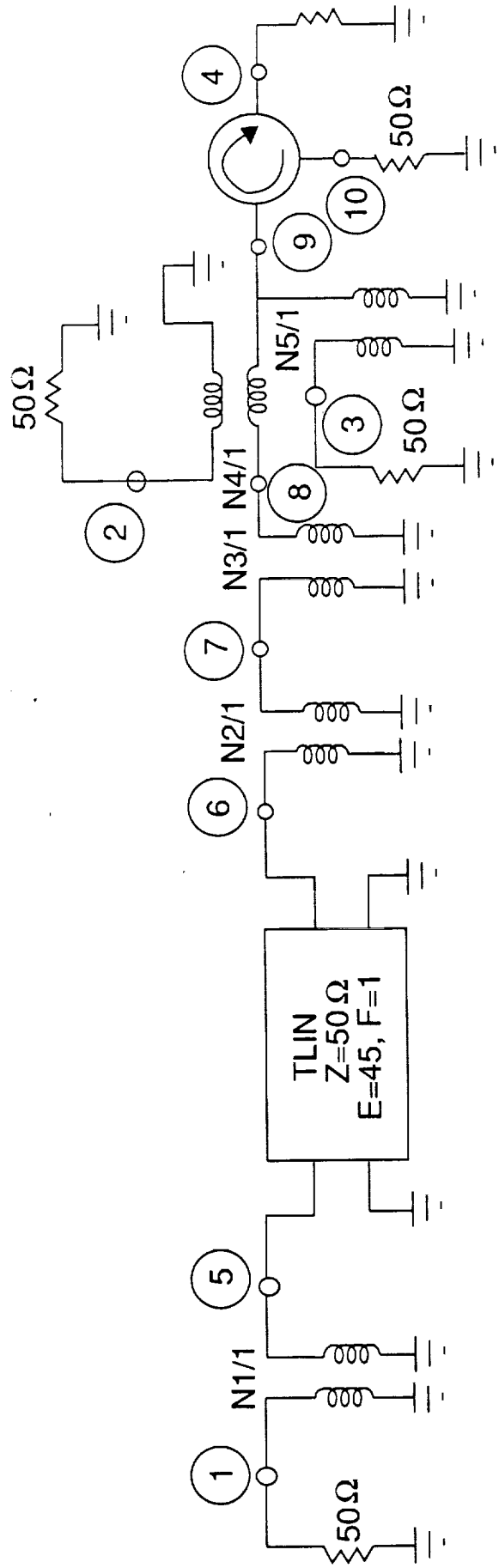

Figure 11. Four/five port simulation of lossy calibration system with ideal circulator.